Hindawi
Bioinorganic Chemistry and Applications
Volume 2023, Article ID 3754561, 15 pages
https://doi.org/10.1155/2023/3754561

Research Article

Moxifloxacin Metal Complexes: Synthesis, Characterisation, Antimicrobial and Antidiabetic Activities with Docking Studies

Sajjad Ali,[1,2,3] Huaiji Zheng,[1] Asma Zaidi,[2] Farhan Ahmed Khan,[2] Syed Majid Bukhari,[2] Muhammad Riaz,[4] Muhammad Mumtaz Khan,[5] Shehla Sammi,[3] Inham u-llah,[3] Ammad Amin,[3] and Muhammad Jahangir[3]

[1]*Shaanxi Key Laboratory of Natural Products and Chemical Biology, College of Chemistry and Pharmacy, Northwest A&F University, 3 Taicheng Road, Yangling 712100, China*
[2]*Department of Chemistry, COMSATS University Islamabad, Abbottabad Campus, Abbottabad 22060, KPK, Pakistan*
[3]*Department of Food Science and Technology, The University of Haripur, Haripur, KPK, Pakistan*
[4]*Department of Basic and Applied Chemistry, Faculty of Science and Technology, University of Central Punjab, Lahore 54000, Pakistan*
[5]*Department of Microbiology, The University of Haripur, Haripur, KPK, Pakistan*

Correspondence should be addressed to Huaiji Zheng; hjzheng@nwsuaf.edu.cn and Muhammad Jahangir; m.jahangir@uoh.edu.pk

Received 18 July 2022; Revised 6 October 2022; Accepted 13 December 2022; Published 3 January 2023

Academic Editor: Massimiliano F. Peana

Six new metal complexes of Fe(III), Cu(II), and Hg(II) were synthesised, i.e., three (2, 4, and 5) with moxifloxacin (mono-ligand) and the other three (1, 3 and 6) with moxifloxacin and hydrazine (biligand). These were characterised through UV-Vis, FT-IR, elemental analysis (CHN), atomic absorption spectroscopy, TGA, scanning electron microscopy (SEM), and powder XRD studies. Further, all of these compounds were screened for their antimicrobial, cytotoxic, and antidiabetic potential. The study revealed that the synthesised metal complexes possess an excellent ability to become antifungal agents compared to moxifloxacin. Additionally, the cytotoxicity of compounds 1, 3, and 4 was in the acceptable range with much better antidiabetic potential as compared to the ligand moxifloxacin. Interestingly, the α-amylase inhibition activity of complexes 1 and 3 was found very close to the standard drug acarbose. Furthermore, the computational studies also authenticate the results of the antidiabetic potential of complexes 1, 3, and 4 by presenting the necessary interactions of these compounds with their respective binding sites. The overall results indicate that the antifungal and antidiabetic ability of moxifloxacin is enhanced significantly by complexation with the given metals and the secondary ligand, thereby making it a suitable lead compound for yet another avenue of an antifungal and antidiabetic agent in the field of drug discovery and development.

1. Introduction

The moxifloxacin hydrochloride [1-cyclopropyl-7-(S,S)-2,8-diazabicyclo(4.3.0)-non-8-yl-6-fluoro-8-methoxy-1,4-dihydro-4-oxo-3-quinoline carboxylic acid hydrochloride] is a new 8-methoxy derivate of fluoroquinolone [1, 2]. It represents one of the recent and influential classes of fourth-generationbroad-spectrum fluoroquinolone antibiotics [3, 4]. Moxifloxacin (Figure 1) is not only active against common Gram-positive and Gram-negative bacteria but also useful against various anaerobes [2, 5]. Studies also show its effectiveness in *tuberculosis* and complicated intra-abdominal infection [6, 7]. Although the synthesis of new quinolone-based antibiotics usually results in increased antimicrobial effects when compared with their respective quinolones, numerous bacterial strains have recently been reported to develop resistance against such drugs [3, 8].

In the past two decades, in search of producing new antimicrobial agents, the thought of metalloantibiotics has been pushed forward with encouraging results, which

divulge that they can play a significant role in improving the biological activities of antibiotics [3, 9–12]. These metal-drug chelates are known to possess antibacterial, fungicidal, and antiviral activities, as well as anticancer and antituberculosis activities. Moreover, the latest studies also show their effectiveness against coronavirus (COVID-19) [9, 13, 14]. In the last few years, several metals in variable molar ratios have been reported for synthesising different mono, binary, and ternary complexes with moxifloxacin [15–19]. These metallic complexes of moxifloxacin are known to possess antibacterial, fungicidal [16, 17, 20], antiviral, antituberculosis, and anticancer activities [9, 10, 18, 19]. In several cases, most of these compounds have been reported as better antimicrobial agents than the respective chelating agents [7, 9, 15, 20]. For instance, zinc, iridium, platinum, osmium, ruthenium, gold, and rhenium metal complexes have also been reported as suitable in luminescent sensing and bio-sensing or chemosensing applications [21, 22].

Hydrazine and its derivatives are major ingredients in the composition of many drugs. It is a very good ligand and chelating agent; it forms a hydrazone group by reacting with carbonyl compounds. Hydrazone groups further have enormous applications in bio-sciences, material sciences, and coordination chemistry due to their capacity to make a variety of stable complexes [23–25]. That is why in the current research work, we, for the first time, utilize hydrazine as a secondary ligand for the complexation of fluoroquinolone antibiotics. Due to vast pharmacological applications and increasing demand for metalloantibiotics, in the present study, we synthesised six new moxifloxacin-metal and moxifloxacin-hydrazine-metal complexes with Fe(III), Cu(II), and Hg(II). The main objectives were synthesising the novel mono and binary ligand metal complexes of moxifloxacin, and evaluating its impact on improvements in cytotoxicity, antibacterial, antifungal, and antidiabetic potential of this drug. Besides this, molecular docking studies were carried out as an evidence-based approach to understanding the mechanism of action and potential active sites of new organometallic molecules as antidiabetic agents.

2. Materials and Methods

2.1. Chemicals and Solvents. The metal salts, $FeCl_3.6H_2O$, $HgCl_2$, $Cu(NO_3)_2.3H_2O$, and NaOH, were purchased from Fluka Chemicals. The hydrazine hydrate (80%) was procured from PanReac AppliChem ITW Reagents. The moxifloxacin hydrochloride, α-amylase, acarbose, solvents (CH_3OH and DMSO), and other chemicals were obtained from Sigma-Aldrich Chemicals Co. All the chemicals and solvents were of analytical grade and used without further purification.

2.2. Synthesis of Moxifloxacin Metal (Mono-Ligand) Complexes. Three mono-ligand moxifloxacin metal complexes were synthesised with minor modifications to the previously reported procedure. The methanolic solution (1 mmol) of moxifloxacin hydrochloride was initially treated

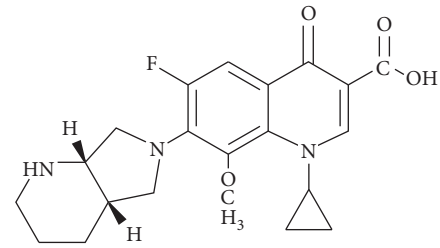

Figure 1: Structure of moxifloxacin.

with a 0.5 M solution of NaOH, and the pH was maintained between 6.3 and 6.5. The clear solution (1 mmol) of each metal, dissolved separately in the same solvents, was added drop-wise to moxifloxacin solutions with continuous stirring until precipitates were obtained. In certain cases where no precipitation occurred, mixtures were stirred for 8 h and left overnight, and the subsequent settled-down solid mass at the bottom was obtained [10, 18, 26, 27].

2.3. Synthesis of Moxifloxacin-Hydrazine Metal (Biligand) Complexes. For mixed ligand metal complexes, the second ligand (hydrazine) was added to the mixture after adding metal salt solution, followed by the same procedure as mentioned above. The resultant filtrates obtained in both cases were initially washed with ice-cold methanol followed by washing with distilled water; the precipitates were dried and kept in air-tight vials [10, 15, 18]. A similar procedure with slight changes in stirring time was repeated to synthesise all new metal complexes. The methodology for synthesising both mono- and biligand metal complexes is summarised in Scheme 1.

3. Characterisation of New Metal Complexes

3.1. UV-Visible Spectroscopy. The μM solutions of all the metal complexes under investigation were prepared in dimethyl sulfoxide (DMSO). The absorbance (200–760 nm) of each solution was measured by using a 10 mm quartz cuvette [28, 29] on a PG instrument, T80+ UV-Vis spectrophotometer.

3.2. X-Ray Diffraction (XRD) Studies. Although the new metal complexes were soluble in common organic solvents, they showed very good solubility in DMSO [30]. Due to the unavailability of proper crystals for a single crystal study, the structures of new organometallic compounds were confirmed by a powder X-ray diffraction technique with a Bruker-D8X-ray (CuKα ($\lambda = 1.5406$ Å) radiation) diffractometer (Brags angle $2\theta = 0$–80°).

3.3. Fourier Transform Infrared (FT-IR) Spectroscopy. The Fourier transform infrared spectra of all the synthesised metal complexes were recorded from 4000 cm^{-1} to 600 cm^{-1} on a Thermo-Nicolet 6700 FT-IR spectrophotometer (Model 270).

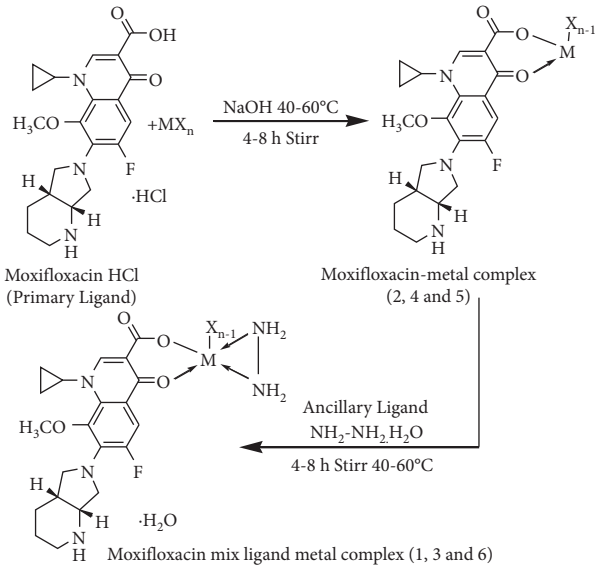

Scheme 1: Synthesis of moxifloxacin metal complexes ($MX_n = FeCl_3.6H_2O$, $HgCl_2$, and $Cu(NO_3)_2.3H_2O$).

3.4. Elemental Analysis. The elemental (C, H, and N) composition of newly prepared metal-drug chelates was assayed with an elemental analyser (Euro Vector Instruments, Euro EA 3000). The atomic absorption spectrophotometer (AA-6300, SHIMADZU) was used for confirmation of the percentage of presence of metal ions.

3.5. Scanning Electron Microscopy (SEM) Analysis. The morphology of moxifloxacin and its metal complexes was examined by scanning electron microscopy on a JEOL scanning electron microscope, JSM 5910.

3.6. Thermogravimetric Analysis (TGA). The thermograms of all organometallic compounds were recorded on Perkin Elmer's instrument, the TGA 4000 system (100–210 at V/50–60 Hz), from 25 up to 800°C in a dynamic nitrogen atmosphere. The flow rate was kept at 20 mL·min^{-1} at a heating rate of 10°C·min^{-1}. A weight of 10.0–25.0 mg of all samples was used in platinum crucibles [15, 20].

4. Biological Activities

4.1. Antimicrobial Evaluation. The synthesised metal complexes were evaluated for antimicrobial activities by using the Agar well diffusion method [31–34]. Both Gram-positive (*Staphylococcus aureus* and *Bacillus subtilis*) and Gram-negative (*Escherichia coli* and *Pasteurella multocida*) bacterial species were used to assess the antibacterial potential. All four bacterial strains were cultured on nutrient agar plates with seeding density. The 5.0 μL of each test sample (dissolved in DMSO) was infused on a sterile filter paper and placed on seeded discs. The positive control of moxifloxacin was also prepared similarly and used as a standard, whereas DMSO-infused discs were used as a negative control. The inhibition zone for each sample and both controls was measured after 24 h incubation at 37°C. For the estimation of antifungal activity, four different fungal stains, *Aspergillus flavus*, *Alternaria alternata*, *Rhizoctonia solani,* and *Aspergillus niger,* were assayed with a similar procedure for antibacterial assay [31, 33].

4.2. Cytotoxic Studies by Hemolytic Activity. The cytotoxicity of new metal complexes was determined by measuring the hemolytic activity. For this purpose, 3 mL of freshly obtained heparinised human blood was centrifuged for 5 min at 850 rpm into a 15 mL striate polystyrene screw cap tube. The resultant floating mass was poured off and washed three times with an ice-cold sterile isotonic phosphate buffered saline (PBS) solution of pH 7.4. The red blood cells were suspended in 20 mL of the same solution (PBS) and counted using a hemocytometer. The obtained blood cell suspension was diluted for each assay with sterile PBS. Then, 20 μL of each sample (metal complex) solution was placed aseptically into 2.0 mL microcentrifuge tubes, and 180 μL of diluted blood cell suspension was mixed with each sample. The mixtures in tubes were incubated with stirring (80 revolutions per minute) for 35 min at 37°C, followed by cooling and centrifugation at 1310 rpm for 5 min. A 100 μL of supernatant from each tube was collected separately in 1.5 mL microfuge tubes, followed by the addition of 900 μL sterile and chilled PBS solution to each tube separately. All of the tubes were kept cold on ice after dilution. The absorbance was noted on a spectrophotometer at 576 nm. The Triton X-100 (0.1%) was taken as a positive control and phosphate buffer saline (PBS) as a negative control, whereas moxifloxacin was used as a reference standard. The percentage of hemolytic activity was calculated by the following formula [35–37]:

$$\%\ \text{cytotoxicity} = \frac{\text{Absorbance of sample}}{\text{Absorbance of control}} \times 100. \quad (1)$$

4.3. Antidiabetic Activity. For the estimation of antidiabetic activity of new chelates of moxifloxacin, α-amylase inhibition analysis was performed as the enzyme kinetic assay (DNS method). An equal volume (500 μL) of prepared metal complexes and a 1% starch solution in 20 mM sodium phosphate buffer (pH 6.9) were used for this assay. A total volume of 500 μL from each sample (metal complex) solution was separately mixed with the same volume of already prepared enzyme solution in a test tube and incubated for 10 min at 37°C. Subsequently, 500 μL of 1% starch solution was added to each mixture and further incubated for 15 min at 37°C, followed by the addition of 1 mL of colouring agent 3,5-dinitro-salicylic acid (DNS) to all mixtures. Further incubation was performed in a water bath (at 85°C for 5 min). In the end, all the samples were allowed to cool down to room temperature, each mixture was diluted with 10 ml distilled water, and absorbance (at 540 nm) was noted using a spectrophotometer. A blank solution (containing all the abovementioned reagents, except metal complexes) was prepared similarly. Acarbose, a well-known synthetic α-amylase inhibitor, was used as the reference standard. The

percentage of inhibition was calculated as follows [38]. IC_{50} values were also calculated for the compounds having more than 50% α-amylase inhibition by the nonlinear calibration curve method using the Origin Pro 6.1 software.

$$\%\ \text{enzyme inhibition} = \frac{\text{Absorbance of blank} - \text{absorbance of sample}}{\text{Absorbance of blank}} \times 100. \quad (2)$$

4.4. Molecular Docking Studies. Molecular docking studies of the most active compounds were carried out by the MOE (molecular operating environment) software [39]. The structures of the ligand, moxifloxacin, and its synthesised complexes were made in the ChemDraw Ultra 14 suite, and the energy was minimised in MOE. The crystal structure of the enzyme human pancreatic α-amylase (PDB ID: 2QV4) [40] was retrieved from the Protein Data Bank [41]. Docking of ligand molecules in the active site of the enzyme was carried out by using MOE-Dock. The Triangle Matcher placement method was used with the London dG scoring function. Refinement was carried out using the Induced-Fit method and rescoring by Affinity dG. The maximum number of retainers was 10 during docking. Final poses were selected based on binding energies, RMSD values, and ligand interactions. To obtain 3D docking poses of complexes, the Discovery Studio Visualizer was used [42]. Three-dimensional surface models were depicted through UCSF Chimera 1.11 software [43].

5. Results and Discussion

A total of six (three mono- and three biligand) metal complexes of moxifloxacin were made by the reaction of moxifloxacin with a methanolic solution of three different metal salts (1 : 1), whereas hydrazine was used as an ancillary ligand in the case of the biligand complex. The ratio of both ligands with salt was 1 : 1 : 1. The proposed molecular formulas and physical data of the new metal complexes are summarised in Table 1 [44–46].

5.1. UV-Vis Spectroscopic Analysis of Synthesised Metal Complexes. UV-Vis spectroscopy is a tool that is widely used for explaining the structural aspects of metal complexes [44]. The results of UV-Vis analysis (Table 2) reveal that moxifloxacin as a free ligand has 3 different absorption bands at 290, 330, and 362 nm assigned for charge transfer, $\pi - \pi^*$, and $n - \pi^*$ transitions, respectively. The first band ($\lambda_{max} = 290$) is the characteristics transition band for moxifloxacin with maximum absorption (1.276). But after complexation with metals, the band shift was observed in new complexes due to transitional charge transfer from the ligand to metal ions ($CT_{M\text{-}L}$). A clear shift was also observed for the other two bands (330 and 362 nm) in new metal complexes, owing to $\pi - \pi^*$ and $n - \pi^*$ transitions, respectively. A change in the maximum wavelength absorbed by the metal complexes can be attributed to structural changes that occurred when moxifloxacin reacted with metal salts to yield metal complexes. Hence, these initial results confirm the synthesis of metal complexes [47–49].

5.2. Powder XRD Studies. The powder XRD patterns are used to access the samples' qualitative degree of crystallinity and phase purity [48]. The powder X-ray diffractograms for moxifloxacin ligand are shown in Figure 2 and for synthesised metal complexes are shown in Figure 3. The diffractogram reflects the data set between 0 and 80° (2θ) values, and the peaks are indexed against 2θ values. The diffractograms for moxifloxacin showed clear peaks, indicating its crystalline nature [47]. The X-ray data for prepared complexes exhibit similar features as compared with each other yet were different from that of the ligand moxifloxacin, which indicates their poor crystallinity (i.e., complexed 1, 2, 3, 5, and 6) or amorphousness (compound 4). The molecular structures with optimised geometry for complexes 1–6 are given in Figures S3a–f in the Supplementary Material. The maximum orientation (2θ) was observed at 10.24° (111) for the ligand and at 13.11° (100), 12.98° (100), 12.94° (100), 12.94° (001), and 12.19° (100) for complexes 1, 2, 3, 5, and 6, respectively, and for complex 4 (Figure 3(e)), no distinct peaks were observed. These results were in agreement with the standards of the Joint Committee on powder diffraction standards (JCPDS No. 00-034-0198). Our results are also insignificant in agreement with results previously reported for moxifloxacin and gemifloxacin metal complexes [47, 48].

5.3. FT-IR Analysis. Investigation of the characteristic vibrations, which are distinctive for the coordination mode of quinolones, can be helpful in the recognition of synthesised moxifloxacin metal complexes. It is known that moxifloxacin either acts as a monodentate, bidentate, or bridging ligand [20, 50, 51]. As a result of stretching and bending vibrations of different functional moieties, various absorption bands of different frequencies were obtained [15, 52]. The possible mechanism of complex formation between moxifloxacin and metal cations can be chelation between the ketonic carbonyl and carboxylic groups [50]. Therefore, in the current study, with other functional groups present in compounds, we also concentrated on validating the vibrations of these carbonyl groups. In the FT-IR spectra (Figures S1a–f in the Supplementary Material) of all the synthesised metal complexes of moxifloxacin (Table 3), the transmittance of the carbonyl (C=O) groups (about 1700 cm^{-1}) of the ligand was observed to show a shift towards lower frequencies and two bands for two carbonyl groups were observed in the range of 1450–1650 cm^{-1}. According to the literature, this shift in the wave number of the carbonyl group is evidence that these functional groups are taking part in complex formation [15, 51]. All the spectra showed the distant peaks for other important function groups such as C-N (between 1346 and 1454 cm^{-1}) and C-O

Table 1: Physical data of moxifloxacin and synthesised metal complexes.

Sr. No.	Formula of metal complex/compound	Physical properties		Mol. weight	MP. (°C)
		Colour	Yield		
1	$[Hg(MXF)\ (N_2H_4)]Cl_2.H_2O$	Dark grey	74%	739	>300
2	$[Hg(MXF)]Cl_2$	Yellowish green	81%	689	>300
3	$[Fe(MXF))(N_2H_4)]Cl_3.7H_2O$	Reddish brown	86%	754	>300
4	$[Fe(MXF)]Cl_3.6H_2O$	Dark brown	86%	687	>300
5	$[Cu(MXF)](NO_3)_2.3H_2O$	Light purple	77%	659	294–298
6	$[Cu(MXF)\ (N_2H_4)](NO_3)_2.4H_2O$	Light purple	79%	723	291–295
Ligand	Moxifloxacin (M.X.F.)	Yellowish green	—	401	>300

Table 2: The UV-Vis spectra of ligand moxifloxacin and its metal complexes.

Sr. No.	Metal complex/compound	Abs.	Electronic bands, λ (nm)			
			$CT_{M\text{-}L}$	$\pi - \pi^*$	$n - \pi^*$	d-d
1	$[Hg(MXF)\ (N_2H_4)]Cl_2.H_2O$	1.037	285	328	362	541
2	$[Hg(MXF)]Cl_2$	1.182	296	332	366	—
3	$[Fe(MXF))(N_2H_4)]Cl_3.7H_2O$	1.193	294	331	358	580
4	$[Fe(MXF)]Cl_3.6H_2O$	1.185	292	334	361	611
5	$[Cu(MXF)](NO_3)_2.3H_2O$	1.243	286	330	358	—
6	$[Cu(MXF)\ (N_2H_4)](NO_3)_2.4H_2O$	1.236	299	336	365	—
Ligand	Moxifloxacin (MXF)	1.276	290	330	362	—

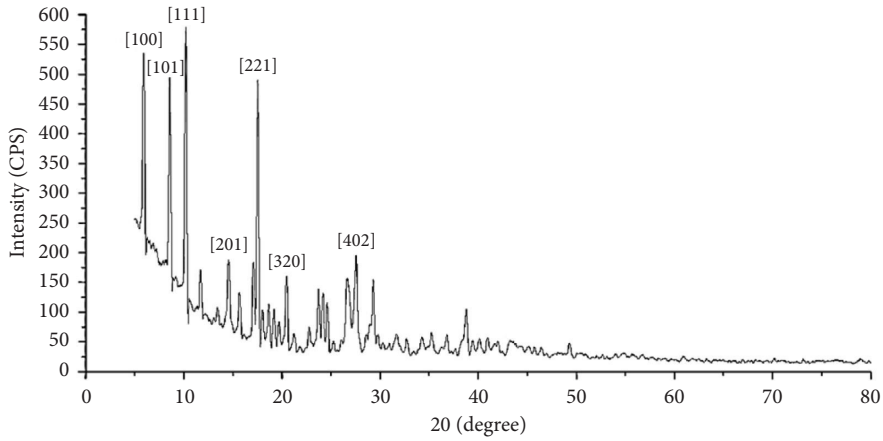

Figure 2: Powder X-ray diffractograms of moxifloxacin.

(between 1029 and 1102 cm^{-1}). The peaks against M-O bonds are also evident in all 6 complexes. Moreover, the new bands at 950 cm^{-1} in the spectra for complex 3 and at 1008 cm^{-1} for complex 4 against the N-N bond also indicate the presence of hydrazine in the muscles. Hence, the values for these two functional groups further confirm the formation of the new metal complexes [16, 44, 53].

5.4. The Elemental (C, H, and N) Analysis. The percentage of carbon, hydrogen, nitrogen, and metal ions in each compound is presented in Table 4. The results indicate that all of the obtained metal complexes 2, 4, and 5 are formed from the reaction of the metal salt with the primary ligand moxifloxacin in a 1 : 1 M ratio and the complexes 1, 3, and 6 in 1 : 1 : 1 of moxifloxacin, metal, and hydrazine, respectively. All complexes except complex 2 are hydrates with various degrees of hydration but are stable solids at room temperature. The results showed significant agreement with the previously reported data in the literature [20, 44, 54] and hence proved the formation of new mixed ligand metal complexes of moxifloxacin.

5.5. SEM Analysis. Figure 4 displays the SEM micrographs of the moxifloxacin and its new complexes. The images were taken in different magnifications, and the micrograph (A) shows that moxifloxacin exhibits a tiny needle-like crystalline morphology. Complexes 1 (B) and 2 (C) possess almost similar sheet-like crystalline structures. Complex 3 (D) exhibits minuscule capsule clusters, while the new organometallic complex 4 (E) showed a powder-like noncrystalline shape. Complex 5 (F) also possesses sheets like aggregates, and complex 6 (G) has nano-sized particles (grown by the process of complexation) of uniform size. The obvious difference in the morphology of

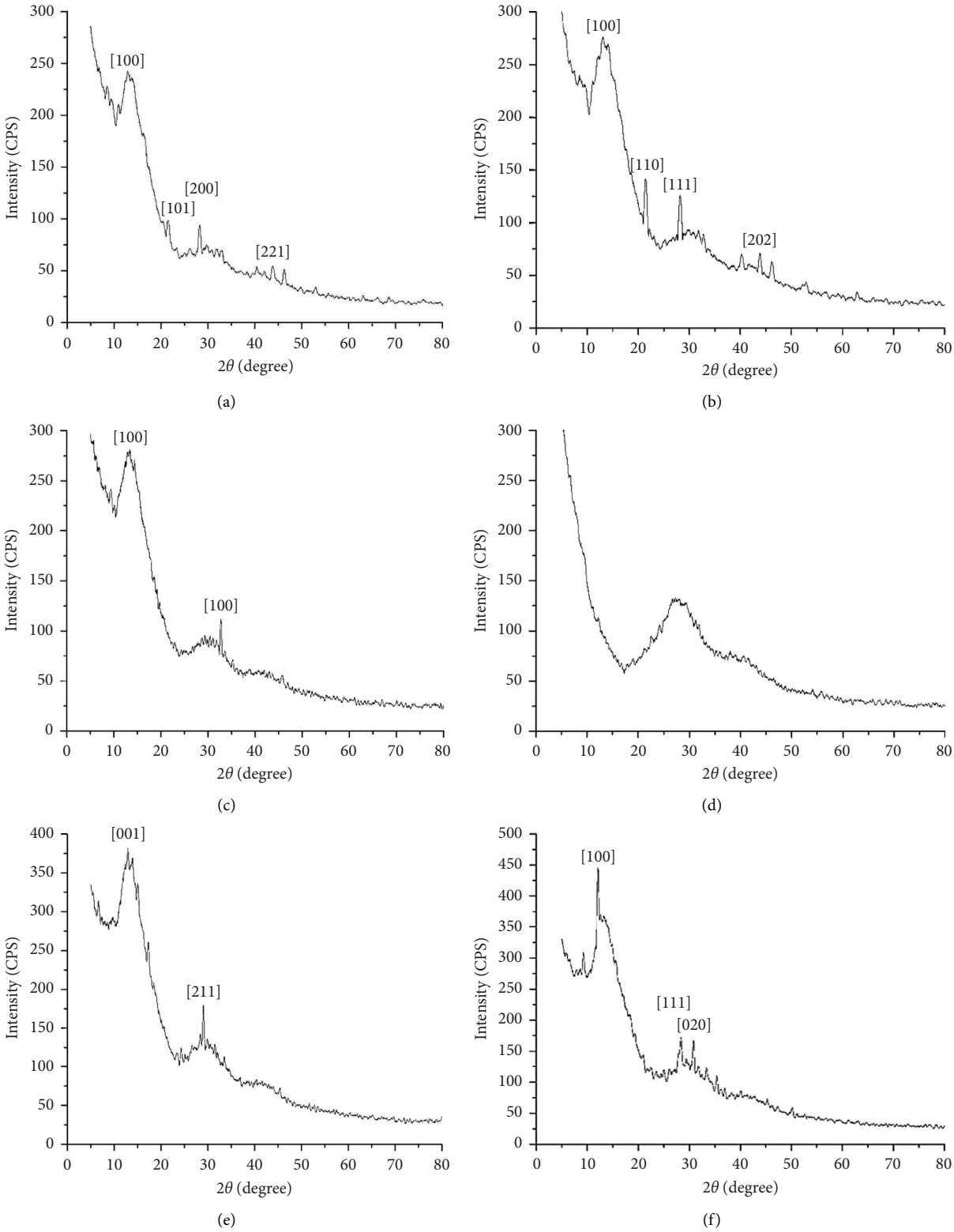

Figure 3: Powder X-ray diffractograms of metal complex 1 to metal complex 6 (a–f), respectively.

Table 3: The FT-IR analysis of moxifloxacin and its new metal complexes (1–6).

Moxifloxacin (ligand)	Metal complex/compound						Assignments
	1	2	3	4	5	6	
2950	—	3064	3042	3050	3153	3183	ν O-H (Ar.)
1725	1612	1623	1616	1623	1635	1645	ν C=O (COOH)
1610	1566	1569	1574	1454	1614	1588	ν C=O
1450	—	1454	1429	1346	1425	1416	ν C-N
1250	1264	1311	1284	1311	1303	1258	ν C-O
1050	1029	1033	1033	1033	1098	1102	ν C-F
—	—	—	950	—	—	1008	ν N–N
—	629	804	623	803	768	719	ν M-O

Table 4: The elemental composition and metal ion content of the isolated solid complexes.

Metal complex	Carbon (%) cal./find	Hydrogen (%) cal./find	Nitrogen (%) cal./find	Metal (%) cal./find
1	36.75/36.88	4.64/4.22	9.48/10.2	27.14/25.68
2	38.35/37.68	4.10/3.96	6.10/5.96	29.11/28.72
3	35.81/34.96	6.28/6.26	9.49/8.86	7.57/8.02
4	38.48/39.02	5.72/6.04	6.12/5.94	8.13/9.14
5	40.09/40.44	5.20/5.32	10.63/11.21	9.64/9.25
6	38.20/38.76	5.85/6.11	13.56/12.83	8.79/8.33

moxifloxacin and its metal complexes clearly indicates the structural modification and formation of new complexes [48, 49, 55].

5.6. Thermogravimetric Analysis (TGA). Thermogravimetric analysis is an analytical technique in which the mass of a fragment is determined either as a function of time or temperature [15]. The results of fragments/mass loss for the six synthesised metal complexes are presented in Table 5, and the thermographs for complexes 1–6 can be found in Figures S2a–f in the Supplementary Material. A two-step degradation pattern has been obtained in the thermal decomposition of the $HgCl_2$ mix legend metal complex. The initial decomposition was observed up to 177°C, which can be characterised as the loss of water for hydration along with the chlorine and methoxy groups. The total weight loss for this phase was 16.6%, close to the experimental result (16.9%). The degradation of the moxifloxacin ligand started next to it and continued up to 350°C, thereby yielding the $C_7H_{14}N_2$ group. The calculated weight loss for this step was 17.3%, whereas the experimental weight loss was 17.5%. Further degradation of the remaining metal complex was not observed. The same decomposition pattern was observed for complexes 2, 3, and 4. In the case of complexes 5 and 6, initially, water loss was observed, followed by the detachment of methoxy and nitro groups up to 197°C. Next, the same group ($C_7H_{14}N_2$) removal was observed, along with fluorine and propyl moiety. In the end, after 242°C, removal of the C_9H_7N group was noted, followed by oxidation of metal above 700°C. Also, hydrazine removal was observed in the thermogravimetric analysis of complex 6 above 200°C. The results for our compounds were found in accordance with the results reported for moxifloxacin metal complexes with Zr, U, and V [44] and comparable to the results reported for the Ti, Y, Pd, Cr, and Zn complexes with moxifloxacin [15, 20, 52].

6. Biological Assays

6.1. Antibacterial Activity. The assayed bacterial strain, *Staphylococcus aureus,* causes food poisoning, skin infection, and respiratory tract infections; *Bacillus subtilis* is found in soil and the gastrointestinal tract of humans but is not pathogenic. In contrast, *Escherichia coli* lives in the intestines of humans and animals and causes diarrhoea. The *Pasteurella multocida* is responsible for various diseases in mammals and birds; it is also known for causing infection (soft tissue inflammation) in the case of dog or cat bites [35, 56, 57]. Figure 5 presents the results for the antibacterial assay. Moxifloxacin (used as a standard) [20] showed pronounced inhibition, counter to all the tested strains. Among all developed compounds, compounds 2 and 5 revealed the most significant activity against *B. subtilis* from the entire tested bacterial strains. Compounds 1 and 3 were selectively active against *P. multocida,* although the activity was proportional to the standard. Compound 4 possessed upright action against *B. subtilis* and *P. multocida* but the highest activity against *E. coli*. The last one, compound 6, showed moderate inhibition, contrary to *B. subtilis* and *E. coli*. In terms of zones of inhibition, compounds 2 (20.0 mm), 4 (26.2 mm), and 5 (20.0 mm) possess not only higher activity than others, but they were even more active than standard against *E. coli.* These results are comparable to the findings reported for mixed ligand complexes of moxifloxacin [20, 58] and gemifloxacin [47] and to different other monoligand complexes of moxifloxacin with various metals [15, 44, 48, 59].

6.2. Antifungal Activity. Moxifloxacin is an effective antibacterial agent similar to other fluoroquinolones, but it is not used as a fungicide in common practice [51]. The results (Figure 6) of the current study disclose that the ligand

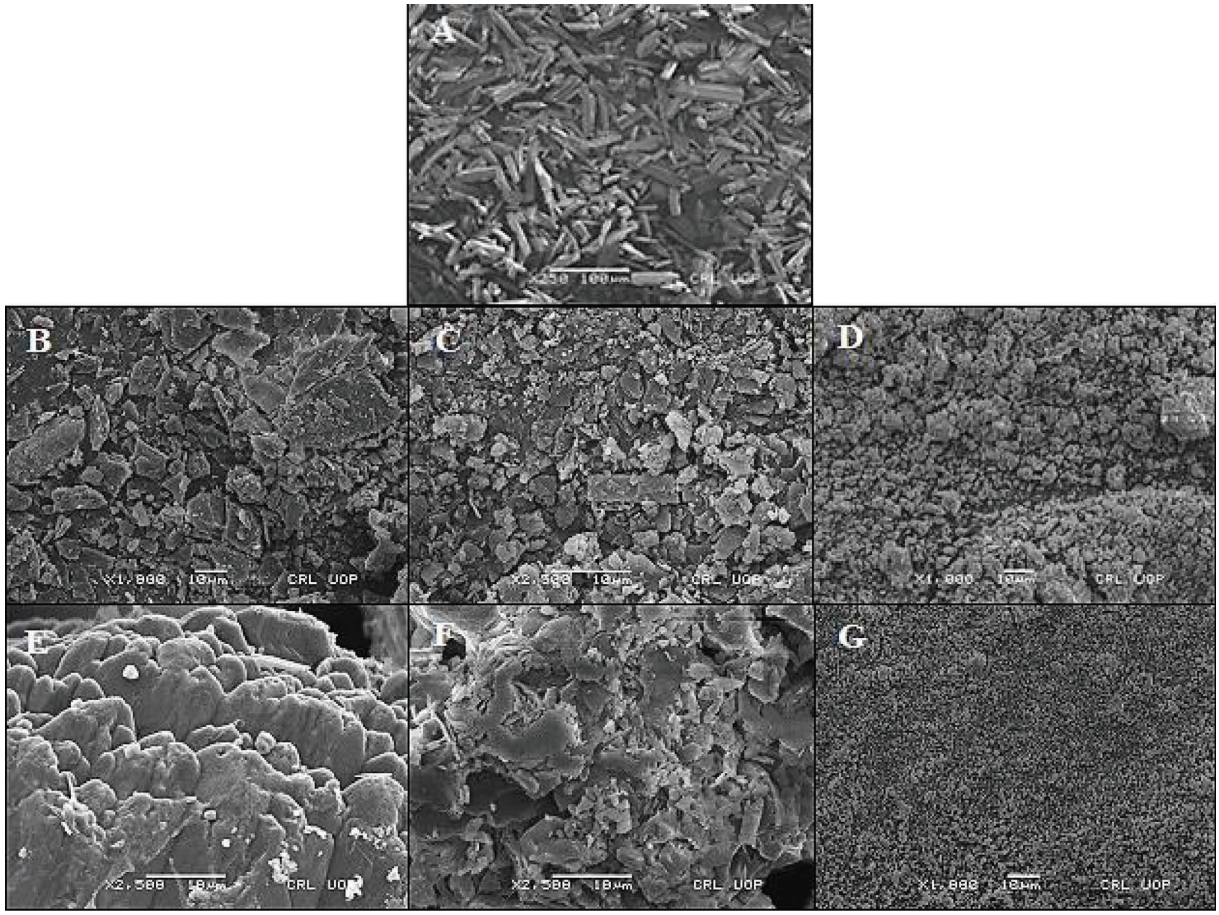

Figure 4: SEM micrographs of moxifloxacin (a) and its metal complexes 1–6 (b–g), respectively.

moxifloxacin was sedentary against *A. flavus* and also exhibited insignificant activities against other fungal strains [59]. Its zones of inhibition for *A. niger*, *R. solani*, and *A. alternata* were 13.4 mm, 7.2 mm, and 6.0 mm, respectively. Compounds 4 and 5 exhibited significantly greater activity against all the screened fungal strains than moxifloxacin. Compounds 1 and 2 present good to modest activity against *A. flavus* and *R. solani*, yet these were inactive against the other two fungi. Compounds 3 and 6 were only inactive against *R. solani*. However, compound 6 possesses not only higher activity against the other three fungal species but is very similar to fluconazole, taken as the standard. It is worth mentioning that almost all the synthesised metal complexes showed substantial antifungal activities against all four fungal strains, except a few. Our results are comparable to the outcomes for moxifloxacin-metal complexes [59] and significantly greater than the antifungal activities reported for mix ligand complexes of moxifloxacin [58]. Therefore, it can be concluded that synthesising metal complexes is an effective step toward modifying moxifloxacin as an antifungal agent, which can serve the purpose of making moxifloxacin considerably active against several fungal species. This development in antifungal activity status can be understood in terms of the implications' concept of cell permeability and Tweed y's chelation theory [59].

6.3. Cytotoxicity. Treating human body cells with a cytotoxic substance can result in different disorders in human beings. The cells of different body tissues can experience a loss of membrane integrity, which may cause cell lysis and the rapid death of cells. The firmness of the cell membrane of red blood cells (RBCs) is a valid indicator to evaluate *in vitro* the effects of several compounds while screening for cytotoxicity [36, 37]. The synthesised organometallic compounds of moxifloxacin with different metals were evaluated *in vitro* for their cytotoxicity by calculating hemolytic activity. The hemolytic activity (Figure 7) of compounds 1–6 was carried out with human red blood cells, and the average RBC lysis was studied for moxifloxacin taken as reference, Triton-X 100 as a positive control, and phosphate buffered saline (PBS) as a negative control [33, 36].

The Triton X-100 shows maximum cell lysis (99.07%), and the negative control shows no (0%) RBC lysis. The ligand moxifloxacin holds very little (6.21%) hemolytic activity. Among the metal complexes, the lowest activity (10.45%) was found for compound 1, and the highest (54.69%) for compound 5. Compounds 3 and 4 showed 16.83% and 12.0% hemolytic activity, respectively, though the cytotoxic values of compounds 1, 3, and 4 are greater than the ligand but are in a safe range for their lead use as

Table 5: The fragments/mass loss of complexes 1–6 at the respective temperature range.

Metal complex	T (°C) max	% loss experimental	% loss calculated	Loss fragments
1	177	16.9	16.6	Cl_2, H_2O, OCH_3
	350	17.5	17.3	$C_7H_{14}N_2$
	—	35.4/64.6	33.9/66.1	
2	180	15.1	15.2	Cl_2, OCH_3
	320	19.2	18.6	$C_7H_{14}N_2$
	—	34.3/65.7	33.8/66.2	
3	186	17.7	17.3	7 H_2O
	320	19.6	19.5	Cl_2, OCH_3
	461	17.5	17.8	$C_7H_{14}N_2$
		55.8/44.2	54.6/45.4	
4	125	15.9	16.1	6 H_2O
	342	21.2	21.5	Cl_2, OCH_3
	378	19.3	18.6	$C_7H_{14}N_2$
	—	56.4/43.6	57.2/42.8	
5	165	10.7	10.9	3 H_2O
	197	15.4	15.6	NO_2, OCH_3
	242	31.0	31.2	$C_7H_{14}N_2$, F, C_3H_5
	358	20.4	20.7	C_9H_7N
	700	21.2	21.5	CuO
	—	98.7/1.3	99.9/0.1	—
6	98	13.8	13.9	4 H_2O
	162	14.5	14.7	NO_2, OCH_3
	198	28.7	28.9	$C_7H_{14}N_2$, F, C_3H_5
	370	23.4	23.8	C_9H_7N, N_2H_4
	700	18.3	18.5	CuO
	—	98.7/1.2	99.0/0.2	—

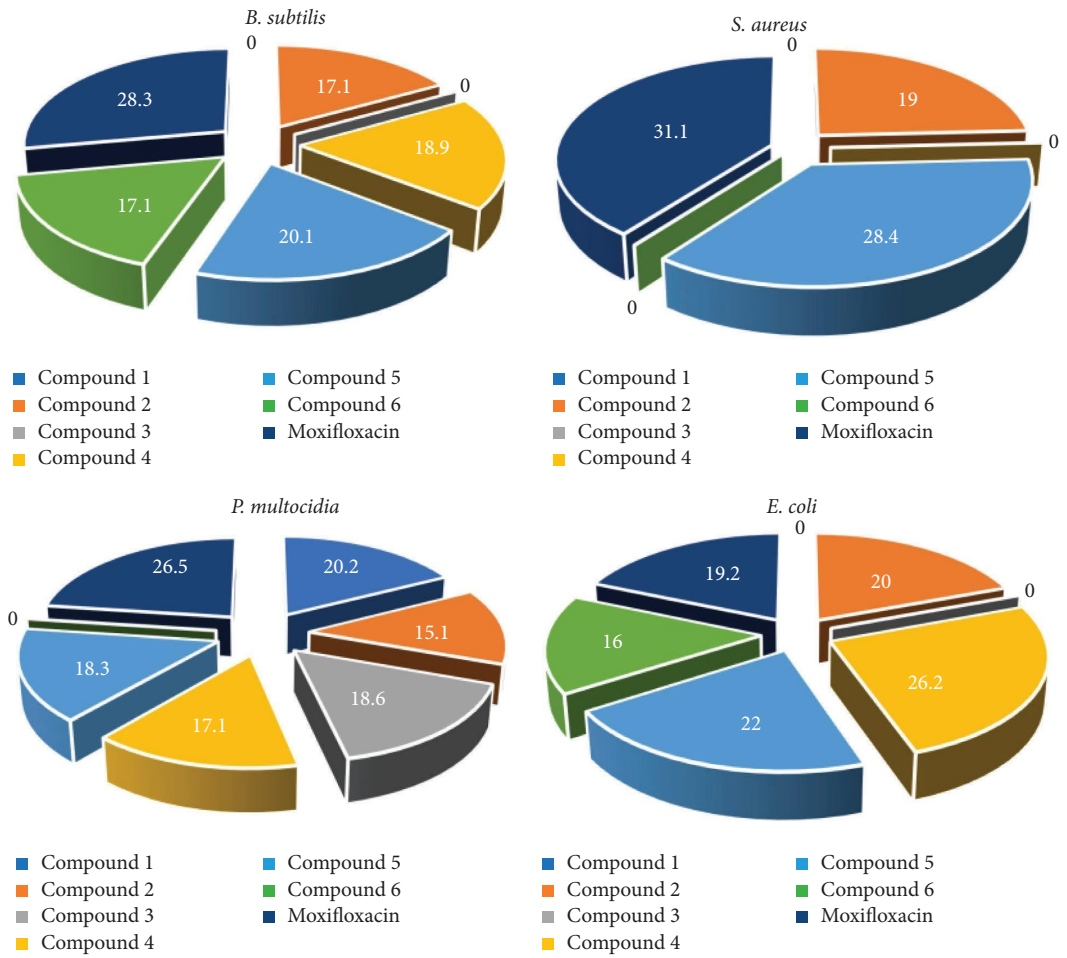

Figure 5: Pie charts representing the extent of antibacterial activities of moxifloxacin and its metal complexes.

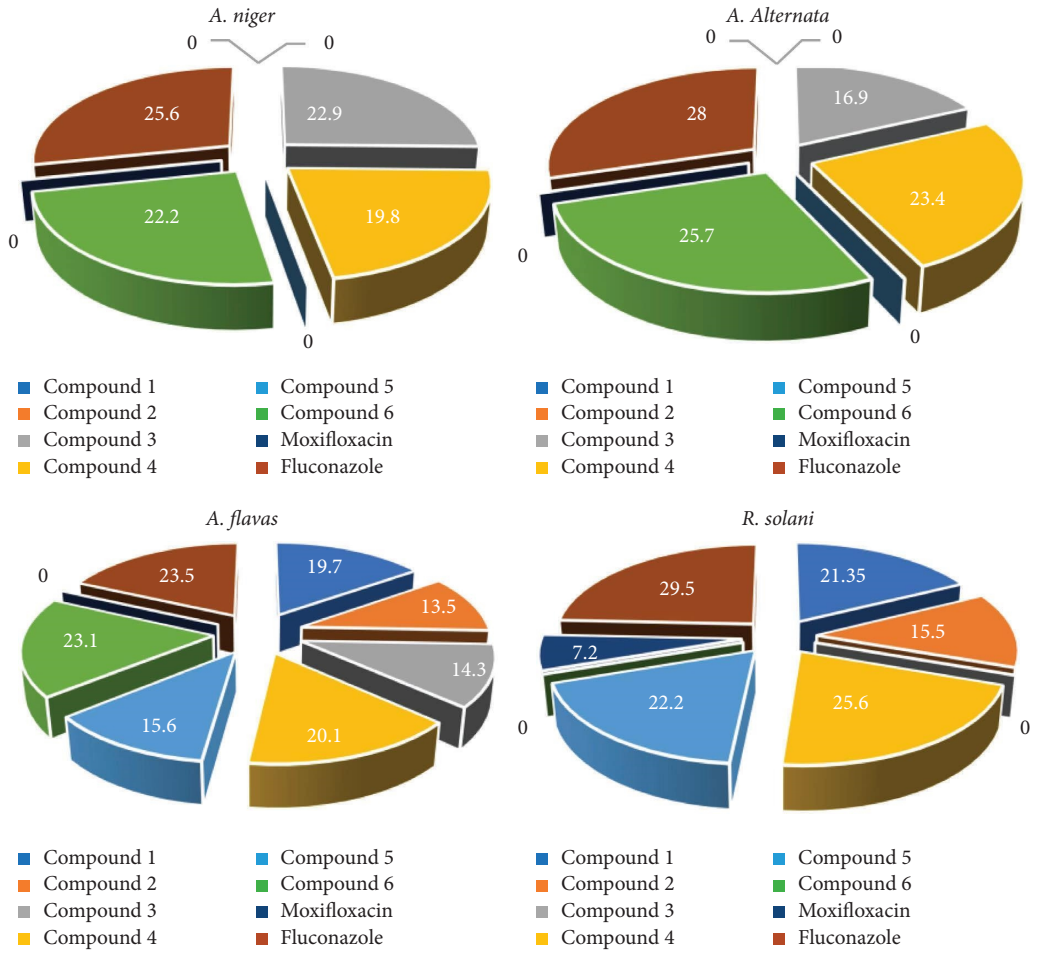

Figure 6: Pie charts representing the extent of antifungal activities of moxifloxacin and its metal complexes.

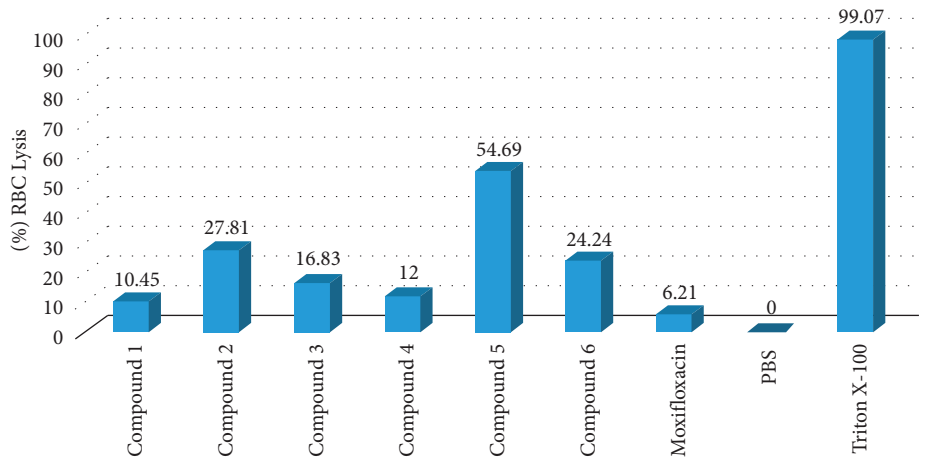

Figure 7: The cytotoxic activity of synthesised metal complexes against moxifloxacin in the presence of positive control (triton X-100) and negative control (PBS).

compounds in the quest for new antibiotics [33]. Our results are comparable to those shown in the literature for the cytotoxicity of similar compounds [37].

6.4. Antidiabetic Activity. Diabetes is one of the world's most rapidly growing metabolic disorders and is also considered a major cause of financial loss in developing countries. There is a need for significant and appropriate drugs in third-world countries to deal with this dreaded disease. Furthermore, unhindered diabetes can lead to several chronic disorders, including blindness, kidney failure, and heart failure [60, 61]. The results for percent antidiabetic activity of all the synthesised metal complexes and IC_{50} values were calculated for compounds 1, 3, and 4 (having more than 50% *α-amylase* inhibition) are summarised in Table 6. The reference standard, acarbose, showed the maximum inhibitory effect (64.12%), and the ligand, moxifloxacin, possessed a minimum (only 3.27%) inhibitory effect. Compound 6 exhibits the lowest (18.48%) antidiabetic activity, whereas compounds 1, 3, and 4 showed the highest (57.33%, 54.15%, and 50.24%, respectively) α-amylase inhibition, which was also close to the standard drug; acarbose. Compounds 2 and 5 also possess significant antidiabetic activity. No previous report on quinolones' metal chelates was found to compare α-amylase inhibition activity. This signifies that the antidiabetic studies of moxifloxacin and its synthesised metal complexes have been carried out for the first time. These results are quite promising and reveal that moxifloxacin can be converted into a drug, thereby treating diabetes if its complexes with suitable metals have been synthesised.

6.5. Molecular Docking Studies. In vitro, α-amylase inhibition results in the current study were further supported by analysing the interactions of synthesised compounds with the active site of α-amylase by performing in silico studies. Binding interactions of the most active compounds 1, 3, and 4 into the active site of human pancreatic α-amylase (PDB ID: 2QV4) [40] were investigated through molecular docking studies using MOE (Molecular Operating Environment) software [39]. Compounds 1, 3, and 4 represented Gibb's free energies (binding energy) of $-14.2\,\text{kcal}\cdot\text{mol}^{-1}$, $-14.8\,\text{kcal}\cdot\text{mol}^{-1}$ and $-12.3\,\text{kcal}\cdot\text{mol}^{-1}$, respectively, with RMSD values of 1.3 Å, 1.8 Å, and 2.5 Å, as given in Table 7. Compounds 1 and 3 represented almost similar interactions compared to the standard drug acarbose by making a conventional hydrogen bond with Gln63, Asp197, Glu233, Asp300, and His305, along with π-alkyl interaction with Trp59 and Leu165 as shown in Figures 8(a) and 8(b). Compound 4 showed less interactions as compared to compounds 1 and 3 (Figure 8(c)), which is also obvious from in vitro studies that compound 4 has less affinity than compounds 1 and 3. A similar type of interaction through molecular docking studies against human α-amylase was observed by Anigboro et al. [62] for plant-based bioactive compounds. The binding pose of compound 1 (pink) into the active site cavity (surface model) of the enzyme along with cocrystallised ligand acarbose (yellow) is shown in Figure 8(d), which indicates that the metal coordination site of moxifloxacin and hydrazine is towards the active site cleft of the enzyme whereas tail is protruding out. Similar binding poses were observed with other compounds. According to the structure-activity relationship (shown in Figure 8), it has been observed that compounds 1 and 3 have more interactions and better affinity as compared to other compounds due to the hydrazine group being coordinated with a metal ion.

Table 6: The % α-amylase inhibition activity and IC_{50} values of synthesised metal complexes, moxifloxacin (ligand) taken as reference, and acarbose taken as standard.

Compound	% α-amylase inhibition	$IC_{50} \pm$ SEM (μM)
1	57.33	441 ± 12
2	39.86	—
3	54.15	463 ± 08
4	50.24	500 ± 05
5	35.68	—
6	18.48	—
References	3.27	—
Standard	64.12	390 ± 10

6.6. Summary. In the present work, six novel metal complexes of Fe(III), Cu(II), and Hg(II) were synthesised. Out of which, three (2, 4, and 5) were with moxifloxacin (monoligand), and the remaining three (1, 3, and 6) were with moxifloxacin and hydrazine (biligand) complexes. The characterisation was done through modern analytical techniques (UV-*Vis*, FT-IR, CHN, AAS, TGA, SEM, and XRD). The prepared organometallic compounds were screened for their antibacterial, antifungal, cytotoxic, and antidiabetic potential. The results revealed that this study is a valuable addition to the literature and has potential application for new drug discovery. An already-developed antibacterial drug (moxifloxacin) has selectively been converted for potent antifungal activity with lower cytotoxicity and a promising candidate to be an antidiabetic drug as a result of chelation. The major outcomes of the research are that compounds 4 and 6 possess significant antifungal activities, and half of the synthesised metal complexes (1, 3, and 4) exhibited potent human pancreatic α-amylase inhibition potential and tolerable cytotoxicity. These compounds should be considered for further development of new antifungal and antidiabetic drugs.

Table 7: Results of docking studies for the most active compounds against human pancreatic α-amylase.

Compound	Binding energy (kcal·mol^{-1})	RMSD (Å)	Residue interactions	
			H-bond	π-alkyl
1	−14.2	1.3	Gln63, Asp197, Glu233, Aps300, His305	Trp59
3	−14.8	1.8	Tyr62 (F), Gln63, Asp197, Glu233, Aps300, His305	Trp59, Leu165
4	−12.3	2.5	Arg195, His299	Trp59, Tyr62
Reference	−9.1	1.6	Arg195, Glu233, His299	—
Standard	Cocrystallized	—	Tyr62, Gln63, Ala106, Thr163, Asp197, Glu233, His299, Aps300, His305	Trp59, His101, Leu165

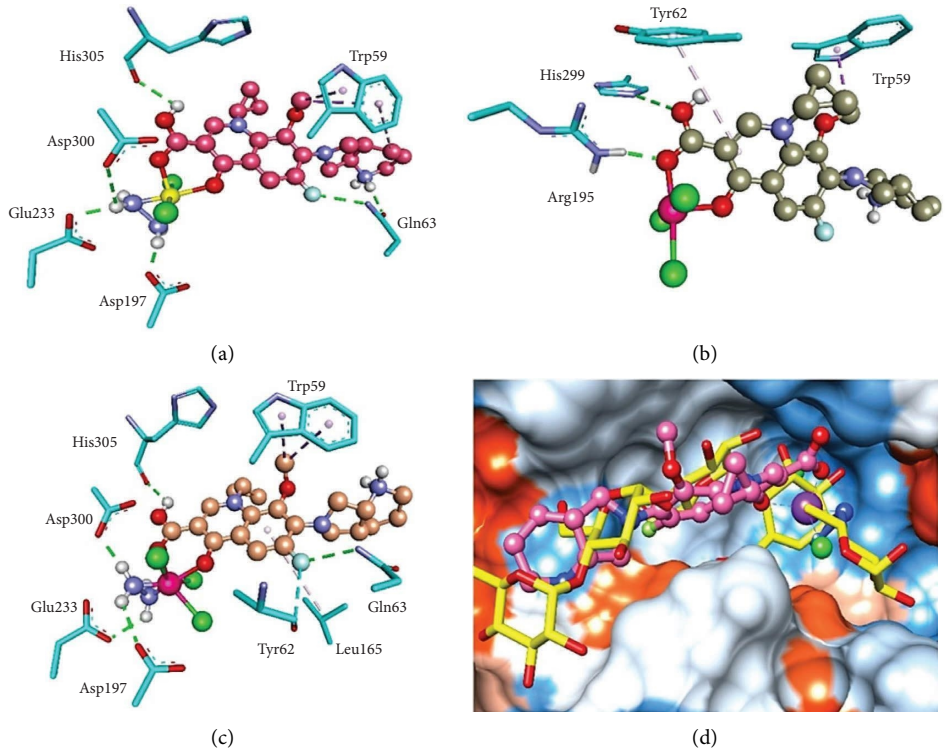

FIGURE 8: The three-dimensional docking poses of compound 1 (a), compound 3 (b), and compound 4 (c) in a ball and stick model are represented in the active site of human α-amylase (PDB ID: 2QV4). The residues are represented in the cyan stick model. The yellow (a), pink (b), and green (c) balls represent Hg, Fe, and Cl, respectively. Green dotted lines represent conventional hydrogen bonds, whereas purple and light purple lines represent π-alkyl interactions. The docking pose of compound 1 (in the pink ball and stick model) and cocrystallised ligand (acarbose in the yellow stick model) are shown in the active site cavity of the enzyme with the hydrophobic surface model (d).

Data Availability

Most of the data supporting the findings of this study are included within the article and the remaining can be found in the Supplementary Materials.

Conflicts of Interest

The authors declare that there are no conflicts of interest.

Acknowledgments

All the authors are grateful to the management of WelWrd Pharmaceutical Industries, Hattar Industrial Estate, Haripur, KPK, Pakistan, for providing research facilities.

Supplementary Materials

Figures S1a–1f: FT-IR spectra of complexes 1–6; Figures S2a–2f: TGA thermographs for complexes 1–6; Figures S3a–f: molecular structures with optimised geometry for complexes 1–6. (*Supplementary Materials*)

References

[1] W. El-Hawary and F. K. Al-Gethami, "Mutual spectrophotometric determination of Moxifloxacin drug and iron (III) ions by formation of a complex compound," *Eur. Chem. Bull*, vol. 2, pp. 22–27, 2012.

[2] H. Stass, A. Dalhoff, D. Kubitza, and U. Schuhly, "Pharmacokinetics, safety, and tolerability of ascending single doses of moxifloxacin, a new 8-methoxy quinolone, administered to healthy subjects," *Antimicrobial Agents and Chemotherapy*, vol. 42, no. 8, pp. 2060–2065, 1998.

[3] S. C. Lopes, C. Ribeiro, and P. Gameiro, "A new approach to counteract bacteria resistance: a comparative study between moxifloxacin and a new moxifloxacin derivative in different model systems of bacterial membrane," *Chemical Biology & Drug Design*, vol. 81, no. 2, pp. 265–274, 2013.

[4] J. M. Blondeau, "Fluoroquinolones: mechanism of action, classification, and development of resistance," *Survey of Ophthalmology*, vol. 49, no. 2, pp. S73–S78, 2004.

[5] E. J. C. Goldstein, D. M. Citron, Y. A. Warren, K. L. Tyrrell, C. V. Merriam, and H. Fernandez, "In vitro activity of moxifloxacin against 923 anaerobes isolated from human intra-abdominal infections," *Antimicrobial Agents and Chemotherapy*, vol. 50, no. 1, pp. 148–155, 2006.

[6] G. Weiss, P. Reimnitz, B. Hampel, E. Muehlhofer, and H. Lippert, "Moxifloxacin for the treatment of patients with complicated intra-abdominal infections (the AIDA Study)," *Journal of Chemotherapy*, vol. 21, no. 2, pp. 170–180, 2009.

[7] S. H. Gillespie, "The role of moxifloxacin in tuberculosis therapy," *European Respiratory Review*, vol. 25, no. 139, pp. 19–28, 2016.

[8] T. D. M. Pham, Z. M. Ziora, and M. A. T. Blaskovich, "Quinolone antibiotics," *Medchemcomm*, vol. 10, no. 10, pp. 1719–1739, 2019.

[9] K. J. Aldred, H. A. Schwanz, G. Li et al., "Overcoming target-mediated quinolone resistance in topoisomerase IV by

introducing metal-ion-independent drug–enzyme interactions," *ACS Chemical Biology*, vol. 8, no. 12, pp. 2660–2668, 2013.

[10] S. Patitungkho, S. Adsule, P. Dandawate, S. Padhye, A. Ahmad, and F. H. Sarkar, "Synthesis, characterization and anti-tumor activity of moxifloxacin–copper complexes against breast cancer cell lines," *Bioorganic & Medicinal Chemistry Letters*, vol. 21, no. 6, pp. 1802–1806, 2011.

[11] Y. Li, J. Dong, P. Zhao et al., "Synthesis of amino acid Schiff base nickel (II) complexes as potential anticancer drugs in vitro," *Bioinorganic Chemistry and Applications*, vol. 2020, Article ID 8834859, 2020.

[12] A. M. Abu-Dief, R. M. El-khatib, S. M. E. Sayed et al., "Tailoring, structural elucidation, DFT calculation, DNA interaction and pharmaceutical applications of some aryl hydrazone Mn (II), Cu (II) and Fe (III) complexes," *Journal of Molecular Structure*, vol. 1244, Article ID 131017, 2021.

[13] H. M. A. Abd El-Lateef, T. El-Dabea, M. M. Khalaf, and A. M. Abu-Dief, "Development of metal complexes for treatment of coronaviruses," *International Journal of Molecular Sciences*, vol. 23, no. 12, p. 6418, 2022.

[14] A. M. Abu-Dief, L. H. Abdel-Rahman, A. A. Abdelhamid et al., "Synthesis and characterization of new Cr (III), Fe (III) and Cu (II) complexes incorporating multi-substituted aryl imidazole ligand: structural, DFT, DNA binding, and biological implications," *Spectrochimica Acta Part A: Molecular and Biomolecular Spectroscopy*, vol. 228, Article ID 117700, 2020.

[15] S. A. Sadeek, W. H. El-Shwiniy, and M. S. El-Attar, "Synthesis, characterization and antimicrobial investigation of some moxifloxacin metal complexes," *Spectrochimica Acta Part A: Molecular and Biomolecular Spectroscopy*, vol. 84, no. 1, pp. 99–110, 2011.

[16] S. A. Sadeek and W. H. El-Shwiniy, "Preparation, structure and microbial evaluation of metal complexes of the second generation quinolone antibacterial drug lomefloxacin," *Journal of Molecular Structure*, vol. 981, no. 1-3, pp. 130–138, 2010.

[17] C. Akinremi, J. Obaleye, S. Amolegbe, J. Adediji, and M. Bamigboye, "Biological activities of some Fluoroquinolones-metal complexes," *International Journal of Medicine and Biomedical Research*, vol. 01, pp. 24–34, 2012.

[18] R. Singh, R. N. Jadeja, M. C. Thounaojam, T. Patel, R. V. Devkar, and D. Chakraborty, "Synthesis, DNA binding and antiproliferative activity of ternary copper complexes of moxifloxacin and gatifloxacin against lung cancer cells," *Inorganic Chemistry Communications*, vol. 23, no. 78-84, pp. 78–84, 2012.

[19] M. J. Feio, I. Sousa, M. Ferreira et al., "Fluoroquinolone–metal complexes: a route to counteract bacterial resistance," *Journal of Inorganic Biochemistry*, vol. 138, pp. 129–143, 2014.

[20] A. A. Soayed, H. M. Refaat, and D. A. Noor El-Din, "Metal complexes of moxifloxacin–imidazole mixed ligands: characterization and biological studies," *Inorganica Chimica Acta*, vol. 406, pp. 230–240, 2013.

[21] K. Kaur, B. Singh, and A. K. Malik, "Chemiluminescence and spectrofluorimetric methods for determination of fluoroquinolones: a review," *Analytical Letters*, vol. 44, no. 9, pp. 1602–1639, 2011.

[22] D. Chakraborty and R. Singh, "Novel fluorescent vanadylmoxifloxacinato complexes as sensors for Cu 2+," *Journal of Photochemistry and Photobiology A: Chemistry*, vol. 335, pp. 211–216, 2017.

[23] S. A. Aly, H. H. Elganzory, M. H. Mahross, and E. M. Abdalla, "Quantum chemical studies and effect of gamma irradiation on the spectral, thermal, X-ray diffraction and DNA interaction with Pd (II), Cu (I), and Cd (II) of hydrazone derivatives," *Applied Organometallic Chemistry*, vol. 35, no. 4, p. e6153, 2021.

[24] S. Aly and S. Fathalla, "Preparation, characterization of some transition metal complexes of hydrazone derivatives and their antibacterial and antioxidant activities," *Arabian Journal of Chemistry*, vol. 13, no. 2, pp. 3735–3750, 2020.

[25] A. M. Abu-Dief, R. M. El-Khatib, F. S. Aljohani et al., "Synthesis, structural elucidation, DFT calculation, biological studies and DNA interaction of some aryl hydrazone Cr3+, Fe3+, and Cu2+ chelates," *Computational Biology and Chemistry*, vol. 97, Article ID 107643, 2022.

[26] R. D. Gosling, L. O. Uiso, N. E. Sam et al., "The bactericidal activity of moxifloxacin in patients with pulmonary tuberculosis," *American Journal of Respiratory and Critical Care Medicine*, vol. 168, no. 11, pp. 1342–1345, 2003.

[27] H. Bensikaddour, N. Fa, I. Burton et al., "Characterization of the interactions between fluoroquinolone antibiotics and lipids: a multitechnique approach," *Biophysical Journal*, vol. 94, no. 8, pp. 3035–3046, 2008.

[28] A. Cirić, R. Jelić, L. Joksović, M. Jelikić-Stankov, and P. Djurdjević, "Determination of moxifloxacin in human plasma by derivative UV spectrophotometry in a micellar medium," *Canadian Journal of Analytical Sciences and Spectroscopy*, vol. 52, pp. 343–350, 2007.

[29] N. E. El-Gamel and M. Zayed, "Synthesis, structural characterization and antimicrobial activity evaluation of metal complexes of sparfloxacin," *Spectrochimica Acta Part A: Molecular and Biomolecular Spectroscopy*, vol. 82, no. 1, pp. 414–423, 2011.

[30] N. G. Yernale and M. Bennikallu Hire Mathada, "Synthesis, characterization, antimicrobial, dna cleavage, and in vitro cytotoxic studies of some metal complexes of schiff base ligand derived from thiazole and quinoline moiety," *Bioinorganic Chemistry and Applications*, vol. 2014, Article ID 314963, 17 pages, 2014.

[31] A. M. Abu-Dief, L. H. Abdel-Rahman, and A. A. H. Abdel-Mawgoud, "A robust in vitro anticancer, antioxidant and antimicrobial agents based on new metal-azomethine chelates incorporating Ag (I), Pd (II) and VO (II) cations: probing the aspects of DNA interaction," *Applied Organometallic Chemistry*, vol. 34, no. 2, Article ID e5373, 2020.

[32] E. T. Aljohani, M. R. Shehata, F. Alkhatib, S. O. Alzahrani, and A. M. Abu-Dief, "Development and structure elucidation of new VO2+, Mn2+, Zn2+, and Pd2+ complexes based on azomethine ferrocenyl ligand: DNA interaction, antimicrobial, antioxidant, anticancer activities, and molecular docking," *Applied Organometallic Chemistry*, vol. 35, no. 5, Article ID e6154, 2021.

[33] S. Hussain, S. Ali, S. Shahzadi, M. N. Tahir, and M. Shahid, "Synthesis, characterization, biological activities, crystal structure and DNA binding of organotin (IV) 5-chlorosalicylates," *Journal of Coordination Chemistry*, vol. 68, no. 14, pp. 2369–2387, 2015.

[34] F. S. Aljohani, A. M. Abu-Dief, R. M. El-Khatib et al., "Structural inspection for novel Pd (II), VO (II), Zn (II) and Cr (III)-azomethine metal chelates: DNA interaction, biological screening and theoretical treatments," *Journal of Molecular Structure*, vol. 1246, Article ID 131139, 2021.

[35] M. Riaz, R. Nasir, H. B. Iftikhar et al., *African Journal of Microbiology Research*, vol. 06, pp. 5700–5707, 2012.

[36] M. Riaz, N. Rasool, I. Bukhari et al., "In vitro antimicrobial, antioxidant, cytotoxicity and GC-MS analysis of Mazus goodenifolius," *Molecules*, vol. 17, no. 12, pp. 14275–14287, 2012.

[37] R. Singh, R. N. Jadeja, M. C. Thounaojam, R. V. Devkar, and D. Chakraborty, "Synthesis, characterization, DNA binding and cytotoxicity studies of moxifloxacinato complexes," *Transition Metal Chemistry*, vol. 37, no. 6, pp. 541–551, 2012.

[38] J. E. Philip, M. Shahid, M. Prathapachandra Kurup, and M. P. Velayudhan, "Metal based biologically active compounds: design, synthesis, DNA binding and antidiabetic activity of 6-methyl-3-formyl chromone derived hydrazones and their metal (II) complexes," *Journal of Photochemistry and Photobiology B: Biology*, vol. 175, pp. 178–191, 2017.

[39] C. C. G. Inc, "Molecular operating environment (MOE)," Chemical Computing Group ULC, Montreal, QC, Canada, 2021.

[40] R. Maurus, A. Begum, L. K. Williams et al., "Alternative catalytic anions differentially modulate human α-amylase activity and specificity," *Biochemistry*, vol. 47, no. 11, pp. 3332–3344, 2008.

[41] H. M. Berman, J. Westbrook, Z. Feng et al., *The Protein Data Bank, 1999–*, International tables for Crystallography, pp. 675–684, 2006.

[42] D. S. Biovia, *Discovery Studio Visualizer*, p. 936, San Diego, CA, USA, 2017.

[43] E. F. Pettersen, T. D. Goddard, C. C. Huang et al., "UCSF Chimera—a visualization system for exploratory research and analysis," *Journal of Computational Chemistry*, vol. 25, no. 13, pp. 1605–1612, 2004.

[44] S. A. Sadeek, W. H. El-Shwiniy, W. A. Zordok, and E. Kotb, "Spectroscopic studies, thermal analyses and biological evaluation of new V (IV), Zr (IV) and U (VI) moxifloxacin complexes," *Journal of Molecular Structure*, vol. 1006, no. 1-3, pp. 192–209, 2011.

[45] K. Kumar and S. Murugesan, "Synthesis, characterization and anti-bacterial activity of divalent transition metal complexes of hydrazine and trimesic acid," *Journal of Saudi Chemical Society*, vol. 22, no. 1, pp. 16–26, 2018.

[46] A. Wojewódka and J. Bełzowski, "Hydrazine complexes of transition metals as perspective explosives," *Chem*, vol. 65, no. 1, pp. 24–27, 2011.

[47] S. A. Sadeek and S. M. Abd El-Hamid, "Synthesis, spectroscopic, thermal analysis and in vitro biological properties of some new metal complexes with gemifloxacin and 1, 10-phenanthroline," *Journal of Thermal Analysis and Calorimetry*, vol. 124, no. 1, pp. 547–562, 2016.

[48] K. Seku, A. K. Yamala, M. Kancherla, K. Kumar K, and V. Badathala, "Synthesis of moxifloxacin–Au (III) and Ag (I) metal complexes and their biological activities," *Journal of Analytical Science and Technology*, vol. 9, no. 1, p. 14, 2018.

[49] M. S. Refat, H. A. Saad, A. A. Gobouri et al., "Synthesis and spectroscopic characterizations of nanostructured charge transfer complexes associated between moxifloxacin drug donor and metal chloride acceptors as a catalytic agent in a recycling of wastewater," *Journal of Molecular Liquids*, vol. 349, Article ID 118121, 2022.

[50] R. Singh, A. Debnath, D. T. Masram, and D. Rathore, "Synthesis and biological activities of selected quinolone-metal complexes," *Research Journal of Chemical Sciences*, vol. 03, pp. 83–94, 2013.

[51] N. Sultana, M. S. Arayne, and M. Akhtar, "Synthesis and antimicrobial chattels of 1-cyclopropyl-7-[(S, S)-2, 8-diazabicyclo [4.3.0]Non-8-Yl]-6- fluoro-8-methoxy -1, 4-dihydro-4-oxo-3-quinolinecarboxylic acid metal complexes of biological interest," *JSM Chem*, vol. 02, no. 1-6, p. 1007, 2013.

[52] K. Sabitha, C. Sajeeth, and K. Santhi, "Chitosan nanoparticles: a novel vehicle for the enhanced ocular delivery of moxifloxacin HCl," *Research Journal of Pharmaceutical, Biological and Chemical Sciences*, vol. 03, pp. 534–548, 2012.

[53] S. Govindrajan and S. T. Aruna, *Hydrazinium Metal Complexes*, Inorganic Hydrazine Derivatives, John Wiley & Sons Ltd, Chichester, UK, 2014.

[54] H. S. Elshafie, S. H. Sakr, S. A. Sadeek, and I. Camele, "Biological investigations and spectroscopic studies of new moxifloxacin/Glycine-metal complexes," *Chemistry and Biodiversity*, vol. 16, no. 3, Article ID e1800633, 2019.

[55] S. Kondaiah, G. Bhagavanth Reddy, D. Rajesh, and B. Vijayakumr, "Synthesis, characterization and biological activity of moxifloxacin-cu (II) metal complex," *IJETSR*, vol. 4, no. 12, pp. 1138–1145, 2017.

[56] S. Y. C. Tong, J. S. Davis, E. Eichenberger, T. L. Holland, and V. G. Fowler, "*Staphylococcus aureus* infections: epidemiology, pathophysiology, clinical manifestations, and management," *Clinical Microbiology Reviews*, vol. 28, no. 3, pp. 603–661, 2015.

[57] S. Hudault, J. Guignot, and A. Servin, "*Escherichia coli* strains colonising the gastrointestinal tract protect germfree mice against *Salmonella typhimurium* infection," *Gut*, vol. 49, no. 1, pp. 47–55, 2001.

[58] S. M Abd El-Hamid, S. Sadeek, W. Zordok, and N. Rashid, "Spectroscopic properties, molecular structure, anticancer and antimicrobial evaluation of some new moxifloxacin metal complexes in the presence of 1, 10-phenanthroline," *Bulletin of the Chemical Society of Ethiopia*, vol. 34, no. 2, pp. 295–312, 2020.

[59] S. M. El-Megharbel, A. M. A. Adam, A. S. Megahed, and M. S. Refat, "Synthesis and molecular structure of moxifloxacin drug with metal ions as a model drug against some kinds of bacteria and fungi," *Russian Journal of General Chemistry*, vol. 85, no. 10, pp. 2366–2373, 2015.

[60] M. Bnouham M, A. Ziyyat, H. Mekhfi, A. Tahri, and A. Legssyer, "Medicinal plants with potential antidiabetic activity-A review of ten years of herbal medicine research (1990-2000)," *International Journal of Diabetes and Metabolism*, vol. 14, no. 1, pp. 01–25, 2006.

[61] M. van de Venter, S. Roux, L. C. Bungu et al., "Antidiabetic screening and scoring of 11 plants traditionally used in South Africa," *Journal of Ethnopharmacology*, vol. 119, no. 1, pp. 81–86, 2008.

[62] A. A. Anigboro, O. J. Avwioroko, O. A. Ohwokevwo, B. Pessu, and N. J. Tonukari, "Phytochemical profile, antioxidant, α-amylase inhibition, binding interaction and docking studies of Justicia carnea bioactive compounds with α-amylase," *Biophysical Chemistry*, vol. 269, Article ID 106529, 2021.